Electronic Supplementary Material (ESI) for Physical Chemistry Chemical Physics.

Supplementary Information

Shengyuan Wang, Kin Fai Tse, Alena Boyko and Junyi Zhu*

Department of Physics, The Chinese University of Hong Kong, Shatin, New Territory, Hong Kong SAR

Note S1: Results of GaN calculations

Methodology

The GaN calculations are also based on the first-principles calculations. For DFE caluclations in GaN, a 3×3×2 supercell containing 72 atoms and a 2×2×2 Γ-centered Brillouin zone meshing are used. Similarly, we perform a SCAN functional relaxation and subsequent ionic and electronic calculations done by HSE functional with 400 eV plane-wave cutoff energy. Range separation parameter μ is set as 0.2 and mixing ratio is adjusted to 0.285 for HSE functional, slightly different from previous setting [1]. The electrostatic correction is also introduced to reach single dilute limit.

GaN chemical potentials

We also calculate the chemical potentials for GaN under both HSE and SCAN functionals. The restrictions are simplified because of the lack of secondary phases. μ_i for HSE calculations are limited by

$$\begin{gathered} \mu_{\mathrm{i}} \leq 0; \\ \mu_{\mathrm{Ga}} + \mu_{\mathrm{N}} = \Delta H_f(\mathrm{GaN}) = -1.35 \text{ eV}. \end{gathered} \tag{S1}$$

Therefore, Ga-rich condition ($\mu_{\mathrm{Ga}} = 0$ eV, $\mu_{\mathrm{N}} = -1.35$ eV) and Ga-poor condition ($\mu_{\mathrm{Ga}} = -1.35$ eV, $\mu_{\mathrm{N}} = 0$ eV) are derived. Similarly, μ_i for SCAN calculations are limited by

$$\begin{gathered} \mu_{\mathrm{i}} \leq 0; \\ \mu_{\mathrm{Ga}} + \mu_{\mathrm{N}} = \Delta H_f(\mathrm{GaN}) = -1.45 \text{ eV}. \end{gathered} \tag{S2}$$

Then Ga-rich condition ($\mu_{\mathrm{Ga}} = 0$ eV, $\mu_{\mathrm{N}} = -1.45$ eV) and Ga-poor condition ($\mu_{\mathrm{Ga}} = -1.45$ eV, $\mu_{\mathrm{N}} = 0$ eV) are calculated and yield similar results as HSE ones.

Lattice constants and bandgap of GaN

The lattice constants and bandgap for GaN are calculated using PBE, SCAN and HSE functional and compared against experimental values, as shown in **Table S1**. Lattice constants from SCAN agree to experimental value with error of 0.21% in

average, while the error for PBE and HSE is 0.95% and 0.34% respectively. Bandgap underestimation by SCAN is reduced to 35.71% compared with PBE (50.86%). However, HSE with a mixing ratio of 0.285 predicts the accurate bandgap of 3.49 eV. Meanwhile, SHSE gives a bandgap of 3.42 eV, which is a considerable bandgap improvement compared to SCAN results.

DFE calculations in GaN

In addition, DFE of GaN as a function of Fermi energy is calculated by SCAN, SHSE and HSE functional in **Fig. S1**. For each defect, DFE deviation from SHSE is 5~34 meV as shown in Table SII, taken HSE calculations as reference. This error in energy is smaller than typical contribution from finite size effects, which is at the order of 0.1 eV or more[2]. The HSE results are in good agreement with previous HSE research[1]. Meanwhile, SCAN results also show a marginal consistence of DFE as a function of Fermi energy with HSE results. A reasonable DFE agreement for defects V_N, Ga_{int}, N_i and Ga_N has achieved, but 2+, 1+, neutral and 1- charge states of V_{Ga}, and 2+, 1+, neutral and 1– charge states of N_{Ga} yield lower DFE than the HSE results. The DFE deviation is listed in **Table S1**, ranging from 0.058 to 0.52 eV compared to HSE results.

Table S1 A list of GaN lattice constants (Å), bandgap E_g (eV) and DFE difference $\Delta E(D)$ (meV) referred to HSE results.

Functional	a	c	E_g	ΔE (V_{Ga})	ΔE (V_N)	ΔE (Ga_{int})	ΔE (N_{int})	ΔE (Ga_N)	ΔE (N_{Ga})
PBE	3.22	5.24	1.72	/	/	/	/	/	/
SCAN	3.18	5.19	2.25	312	233	58	158	156	519
SHSE	3.18	5.19	3.42	34	18	5	14	33	33
HSE	3.18	5.17	3.49	0	0	0	0	0	0
Experiment (ref) [3]	3.19	5.19	3.51	/	/	/	/	/	/

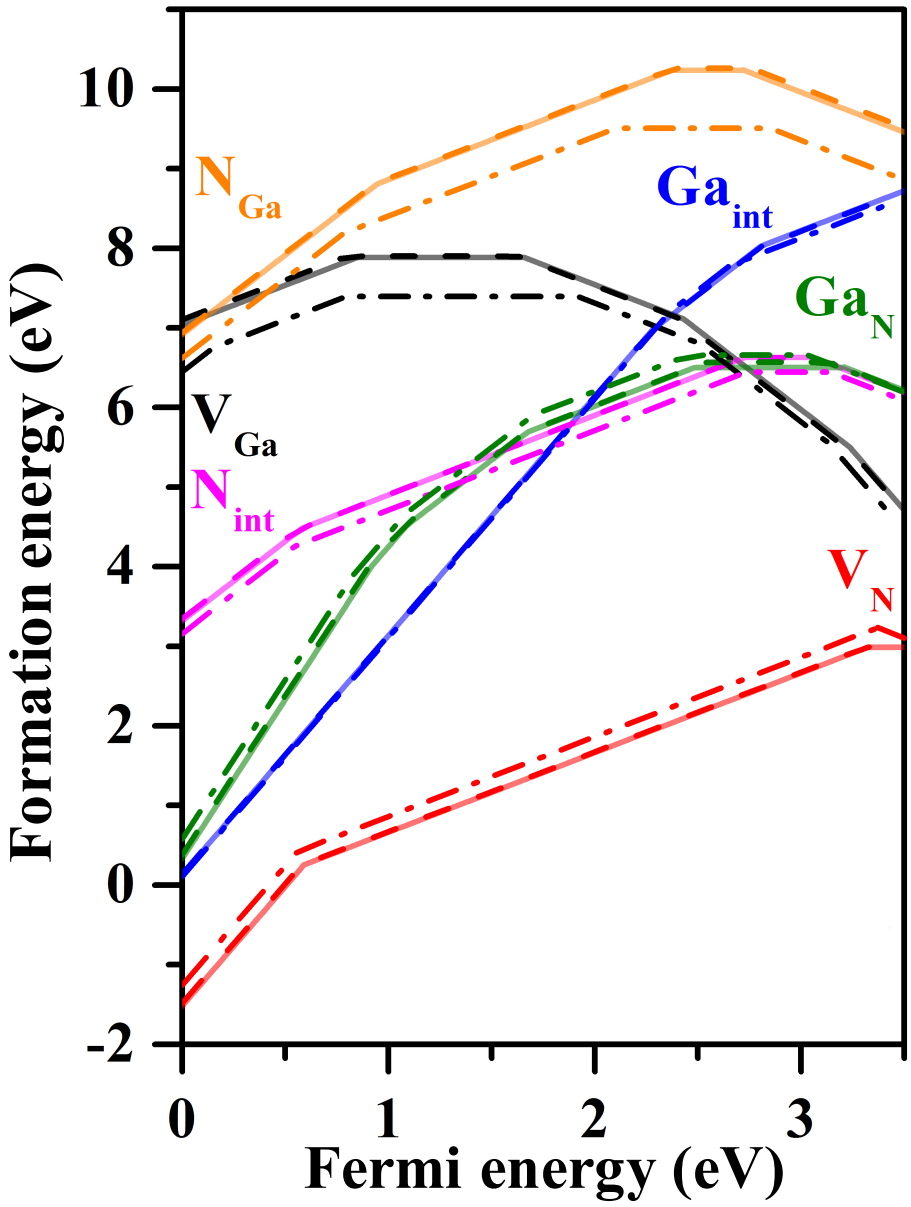

Fig. S1 DFE calculated by SCAN (dash dot line), static HSE (dash line) and HSE functional (solid line) of GaN point defects starting from a SCAN relaxed structure. Rigid shifts of -0.67 and 0.58 eV are added to VBM and CBM of SCAN band edge in order to match HSE bandgap.

Note S2: Detailed calculations of ΔE

Table S2 A list of DFE difference ΔE(D) (meV) and average DFE difference $\overline{\Delta E}$(D) (meV) of V_I, V_{Pb} and V_{Cs} referred to HSE results. The relative errors of DFE of each defect charge state are listed in the bracket. The erroneous charge states are labeled in red.

(1) V_I

Functional	ΔE(V_I) of each charge state			$\overline{\Delta E}$(V_I)
	2+	1+	0	
PHSE	749 (158.75%)	385 (164.51%)	359 (17.53%)	498
SCAN	77 (16.27%)	62 (26.77%)	342 (16.73%)	161
SHSE	397 (84.03%)	217 (92.78%)	252 (12.29%)	289

(2) V_{Pb}

Functional	ΔE(V_{Pb}) of each charge state				$\overline{\Delta E}$(V_{Pb})
	1+	0	1-	2-	
PHSE	81 (4.53%)	62 (3.44%)	159 (7.89%)	71 (2.81%)	93
SCAN	946 (52.89%)	919 (51.37%)	783 (63.86%)	636 (25.20%)	821
SHSE	87 (4.88%)	221 (12.33%)	182 (9.04%)	36 (1.42%)	131

(3) V_{Cs}

Functional	ΔE(V_{Cs}) of each charge state		$\overline{\Delta E}$(V_{Cs})
	0	1-	
PHSE	113 (7.64%)	165 (8.62%)	139
SCAN	159 (10.73%)	198 (10.34%)	179
SHSE	266 (17.94%)	267 (13.97%)	266

Note S3: Detailed comparison of DFE in γ-$CsPbI_3$ between SCAN and HSE results

We firstly calculated the DFE at I-rich condition, as shown in the main text. SCAN functional yields a restricted p-type doping similar to HSE results, yet fails to predict the n-type doping difficulties. V_I^{1+}, V_{Cs}^{1-} and V_{Pb}^{1-} collectively pin the Fermi level at 0.52 eV above VBM with DFE of 0.71 eV, which indicates slightly p-type conductivity, consistent with HSE calculations. There are two stable p-type defects V_{Cs} and I_{Cs} with low DFE of neutral states at 0.90 and 1.44 eV, respectively, indicating a high concentration of p-type defects. In this regard, HSE results give a larger DFE of neutral states of V_{Cs} and the bipolar I_{Cs} properties. V_{Pb} is bipolar in SCAN results, adding a (1+/0) transition level at Fermi level of 0.03 eV above VBM, also different from p-type defect by HSE results. However, the (0/1-) transition levels of V_{Cs} and I_{Cs} are 0.40 and 0.63 eV above VBM that are deep levels, which hinder radiative recombination and restrict the intrinsic p-type doping. Meanwhile, n-type defects V_I, Cs_{int} and Pb_{Cs} introduce (1+/0) transition levels at 1.53, 1.43 and 1.09 eV above VBM with low DFE of neutral states at 1.72, 2.43 and 1.84 eV respectively. These results are different from HSE results which only introduce resonance peaks. The spurious (1+/0) transition levels make intrinsic n-type doping feasible because of the wrong couplings between the defect state and conduction band edge.

Next we calculate DFE under I-medium condition, as shown in the main text, and find that the results of either p-type or n-type is significantly different from HSE ones. V_I^{1+}, V_{Cs}^{1-} and V_{Pb}^{2-} collectively pin the Fermi level at 1.02 eV above VBM with the DFE of 0.77 eV, which indicates slightly n-type conductivity, consistent with HSE results. The p-type defects, V_{Cs} and I_{Cs}, elevate the DFE of neutral states to 1.40 and 2.38 eV, respectively. Meanwhile, n-type defects, V_I, Cs_{int} and Pb_{Cs}, reduce the DFE of neutral states to 1.28, 1.93 and 1.36 eV, respectively. The concentration of p-type (n-type) defects is decreased (increased) with chemical potential shifting from I-rich to I medium condition, consistent with HSE prediction. However, p-type and n-type defects

have comparable low DFE under I-medium condition, which erroneously shows the feasibility of either intrinsic p-type or n-type doping.

Finally, we calculate DFE under I-poor condition, as shown in the main text. The SCAN results exhibit a limited n-type doping similar to HSE results, but fail to demonstrate the p-type difficulties. V_I^{1+}, V_{Cs}^{1-} and V_{Pb}^{2-} collectively pin the Fermi level at 1.46 eV above VBM with the DFE of 0.77 eV, which indicates a good n-type conductivity, consistent with HSE calculations. The n-type defects, V_I, Cs_{int} and Pb_{Cs}, introduce (1+/0) transition levels at 1.53, 1.43 and 1.09 eV above VBM and reduce DFE of neutral states to 0.84, 1.43 and 1.05 eV, respectively. These results suggest a high concentration of n-type carriers. However, the deep levels also hinder the n-type conductivity, consistent to HSE conclusion. Meanwhile, the p-type defects, V_{Cs}, elevates the DFE of neutral states to 1.90 eV. The underestimation of DFE of V_{Cs} erroneously contributes to feasible intrinsic p-type doping, different from the high DFE of V_{Cs} by HSE results.

Note S4: Structural analysis of Pb_I, Pb_{Cs}, Pb_{int} and Cs_I

Structural analysis of Pb_I

For Pb_I, a misestimation of defect displacements and neighboring iodine numbers leads to erroneous stabilization of 1- and 0 states and destabilization of 2+ state by SCAN functional. The schematic local structures of Pb_I by both HSE and SCAN functionals are shown in **Fig. S2(a) and (e)**, respectively. Pb_I is stable in 1+, 2+ and 3+ charge states by HSE functional. In all three charge states, the defect shows significant displacements from its ideal antisite position into the surrounding iodine environment, ranged from 0.62 to 1.72 Å with the largest displacement in Pb_I^{3+} as shown in **Table S3**. The iodine neighbors for each charge state are two, three and four, respectively. The displacement of the defect modifies its neighboring configurations, introduces extra lead-iodine bonds, changes the bond orbital coupling, and results in the complex transition. Similar displacements of the defect into the surrounding iodine environment are also observed in several states by SCAN functional. Specifically, the SCAN results show that the stable 1-, 0, 1+ and 3+ charge states have the displacements of 0.29, 0.60, 0.80 and 1.85 Å with zero, one, two and four iodines as neighbors, respectively. However, the erroneous relaxation in 1- state by SCAN functional leads to one less neighboring iodine than the corresponding HSE configurations. The error stabilizes the 1- state in the bandgap. Similarly, the insufficient relaxation in 2+ state by SCAN functional leads to one less neighboring iodine than the HSE results.

Structural analysis of Pb_{Cs}

For Pb_{Cs}, it is the insufficient relaxation that spuriously stabilizes neutral state in SCAN results. The schematic local structures of Pb_{Cs} by both HSE and SCAN functionals are shown in **Figure S2(b) and (f)**, respectively. HSE functional treats Pb_{Cs} as resonance peaks, and only 1+ state is stable in the bandgap. However, SCAN results show that both 1+ and neutral states are stable. We further find that the displacements are 0.71 and 0.44 Å for 1+ and neutral states in HSE results, respectively, as

demonstrated in **Table S4**. Therefore, the insufficient displacement of the neutral state may lead to a relatively weak coupling between the defect and surrounding iodines and destabilize the neutral state in comparison to 1+ state. However, the displacements of both charge states in SCAN results are small, with 0.22 and 0.21 Å for +1 and neutral states, respectively. The small difference may effectively lead to a stabilization of the neutral state by SCAN functional.

Structural analysis of Pb_{int}

For Pb_{int}, SCAN functional gives a relatively poor structural optimization in 2+ state. The schematic local structures of Pb_{int} by both HSE and SCAN functionals are shown in **Fig. S2(c) and (g)**, respectively. Pb_{int} is stable in both 2+ and 1+ charge states by HSE functional. If we assume the geometric center of the surrounding iodine atoms near the Pb_{int} as the original position, no obvious displacement of the defect is observed in both charge states. However, the number of iodine neighbors is changed from 4 to 6 when the charge state is changed from 1+ to 2+, as exhibited in **Table S5**. The displacement of surrounding two iodine atoms introduces extra lead-iodine bonds in the +2 state, changes the bond orbital coupling, and reduces the DFE. However, SCAN results show that 2+, 1+ and neutral states are stable with displacements of 1.13, 0.01 and 0 Å, respectively. The iodine neighbors for all the charge states are four. Different from HSE results, in the 2+ state by SCAN functional, the defect undergoes an obviously erroneous displacement towards the I6 atom, which removes two neighbors. However, the (2+/1+) transition level by both functionals are similar, which is probably coincidental. In addition, the spurious (1+/0) transition level by SCAN functional is probably due to the band edge error.

Structural analysis of Pb_{Cs}

Similar to Pb_{Cs}, insufficient defect relaxation in Cs_I destabilizes 3+ state in SCAN results. The schematic local structures of Cs_I by both HSE and SCAN functionals are shown in **Fig. S2(d) and (h)**, respectively. Cs_I is stable in 0, 1+, 2+ and 3+ charge states by HSE functional with the displacements of 1.20, 1.31, 1.29 and 1.24 Å, respectively,

as shown in **Table S6**. However, the displacements for 0, 1+, 2+ and 3+ by SCAN functional are 0.99, 0.99, 0.97 and 0.91 Å, respectively. Note that the displacements of various charge states in HSE functional are similar, however, that of 3+ state in SCAN functional is significantly smaller than other states and may destabilize the state effectively.

Table S3. A list of the distances d (Å) between Pb_I and neighbors in 3+, 2+, 1+, 0 and 1- states by both SCAN and HSE functional, the distances between the original iodine and the neighbors in the host cell and the displacements of the defect sites to initial position during the relaxation. Pb_I^0 and Pb_I^{1-} are unstable in HSE results, while Pb_I^{2+} is unstable in SCAN results.

(1) HSE results

Neighbors	d (Pb_I^{3+})	d (Pb_I^{2+})	d (Pb_I^{1+})	d (Pb_I^0)	d (Pb_I^{1-})	d (host)
Pb1	/ (3.72)	3.29	3.12	3.11	3.11	3.23
Pb2	/ (3.98)	/ (3.94)	3.20	3.05	3.06	3.23
I1	3.11	3.20	3.06	3.12	3.12	4.45
I2	2.94	2.97	3.06	/ (4.63)	/ (4.70)	4.56
I3	/ (5.13)	/ (4.86)	/ (4.45)	/ (4.19)	/ (4.17)	4.68
I4	3.43	3.32	/ (4.12)	/ (4.61)	/ (4.59)	4.68
I5	2.95	/ (3.79)	/ (4.28)	/ (4.54)	/ (4.65)	4.57
Displacements	1.72	1.38	0.62	0.49	0.55	0

(2) SCAN results

Neighbors	d (Pb_I^{3+})	d (Pb_I^{2+})	d (Pb_I^{1+})	d (Pb_I^0)	d (Pb_I^{1-})	d (host)
Pb1	/	3.38	3.17	3.17	3.04	3.22
Pb1	/	3.44	3.16	3.09	3.03	3.23
I1	3.04	3.07	3.14	3.27	/ (4.07)	4.56
I2	2.99	3.01	3.10	/ (4.34)	/ (4.61)	4.54
I3	3.44	/ (4.02)	/ (4.25)	/ (4.14)	/ (4.18)	4.52
I4	/ (4.89)	/ (4.26)	/ (4.16)	/ (4.53)	/ (4.64)	4.58
I5	3.11	/ (3.96)	/ (4.29)	/ (4.37)	/ (4.62)	4.58
Displacements	1.85	1.18	0.80	0.60	0.29	0

Table S4. A list of the distances d (Å) between Pb_{Cs} and neighbors in 1+ and 0 states by both SCAN and HSE functional, the distances between the original iodine and the neighbors in the host cell and the defect displacements. Pb_{Cs}^{0} is unstable in HSE results.

(1) HSE results

Neighbors	d (Pb_{Cs}^{1+})	d (Pb_{Cs}^{0})	d (host)
I1	3.30	3.43	3.76
I2	3.23	3.36	3.82
I3	3.22	3.44	4.00
I4	3.26	3.40	3.87
I5	3.09	/ (4.07)	4.32
I6	/ (4.02)	/ (4.29)	4.00
I7	/ (4.12)	/ (3.79)	3.87
Displacements	0.71	0.44	0

(2) SCAN results

Neighbors	d (Pb_{Cs}^{1+})	d (Pb_{Cs}^{0})	d (host)
I1	3.18	3.18	3.89
I2	3.50	3.56	3.89
I3	/ (3.71)	/ (3.79)	4.08
I4	3.20	3.17	3.91
I5	/ (4.51)	/ (4.50)	4.24
I6	3.68	/ (4.07)	4.08
I7	3.20	3.17	3.91
Displacements	0.22	0.21	0

Table S5. A list of the distances d (Å) between Pb_{int} and neighbors in 2+, 1+ and 0 states by both SCAN and HSE functional, the distances between the original iodine and the neighbors in the host cell and the defect displacements. Pb_{int}^{0} is unstable in HSE results.

(1) HSE results

Neighbors	d (Pb_{int}^{2+})	d (Pb_{int}^{1+})	d (Pb_{int}^{0})	d (host)
I1	3.35	/ (4.38)	/ (4.38)	4.60
I2	3.33	/ (4.38)	/ (4.37)	4.60
I3	3.25	3.30	3.31	3.76
I4	3.25	3.30	3.31	3.76
I5	3.17	3.21	3.20	2.59
I6	3.17	3.21	3.20	2.59
Displacements	0.01	0	0	0

(2) SCAN results

Neighbors	d (Pb_{int}^{2+})	d (Pb_{int}^{1+})	d (Pb_{int}^{0})	d (host)
I1	/ (5.95)	/ (4.65)	/ (4.64)	4.76
I2	3.15	/ (4.65)	/ (4.64)	4.76
I3	3.03	3.32	3.34	3.78
I4	/ (3.84)	3.33	3.34	3.78
I5	3.27	3.18	3.18	2.55
I6	3.03	3.19	3.18	2.55
Displacements	1.13	0.01	0	0

Table S6. A list of distances d (Å) between Cs_I and neighboring leads and iodines in 3+, 2+, 1+ and 0 states by both SCAN and HSE functional, the distances between the original iodine and the neighbors in the host cell and the defect displacements. Cs_I^{3+} is not stable in SCAN results.

(1) HSE results

Neighbors	d (Cs_I^{3+})	d (Cs_I^{2+})	d (Cs_I^{+})	d (Cs_I^{0})	d (host)
Pb1	4.23	4.27	4.26	4.06	3.23
Pb2	4.15	4.15	4.12	4.03	3.23
I1	3.92	3.97	4.00	3.92	4.48
I2	4.00	4.05	4.04	3.95	4.45
I3	3.86	3.86	3.85	3.82	4.56
I4	3.96	3.97	3.98	3.95	4.57
I5	3.89	3.86	3.84	3.82	5.18
Displacements	1.24	1.29	1.31	1.20	0

(2) SCAN results

Neighbors	d (Cs_I^{3+})	d (Cs_I^{2+})	d (Cs_I^{+})	d (Cs_I^{0})	d (host)
Pb1	3.93	3.95	3.91	3.89	3.22
Pb2	3.96	3.96	3.91	3.89	3.23
I1	4.10	4.00	4.00	4.00	4.45
I2	4.16	4.15	4.18	4.19	4.56
I3	3.90	3.89	3.88	3.88	4.54
I4	4.10	4.09	4.06	4.06	4.58
I5	3.95	3.90	3.89	3.87	5.10
Displacements	0.91	0.97	0.99	0.99	0

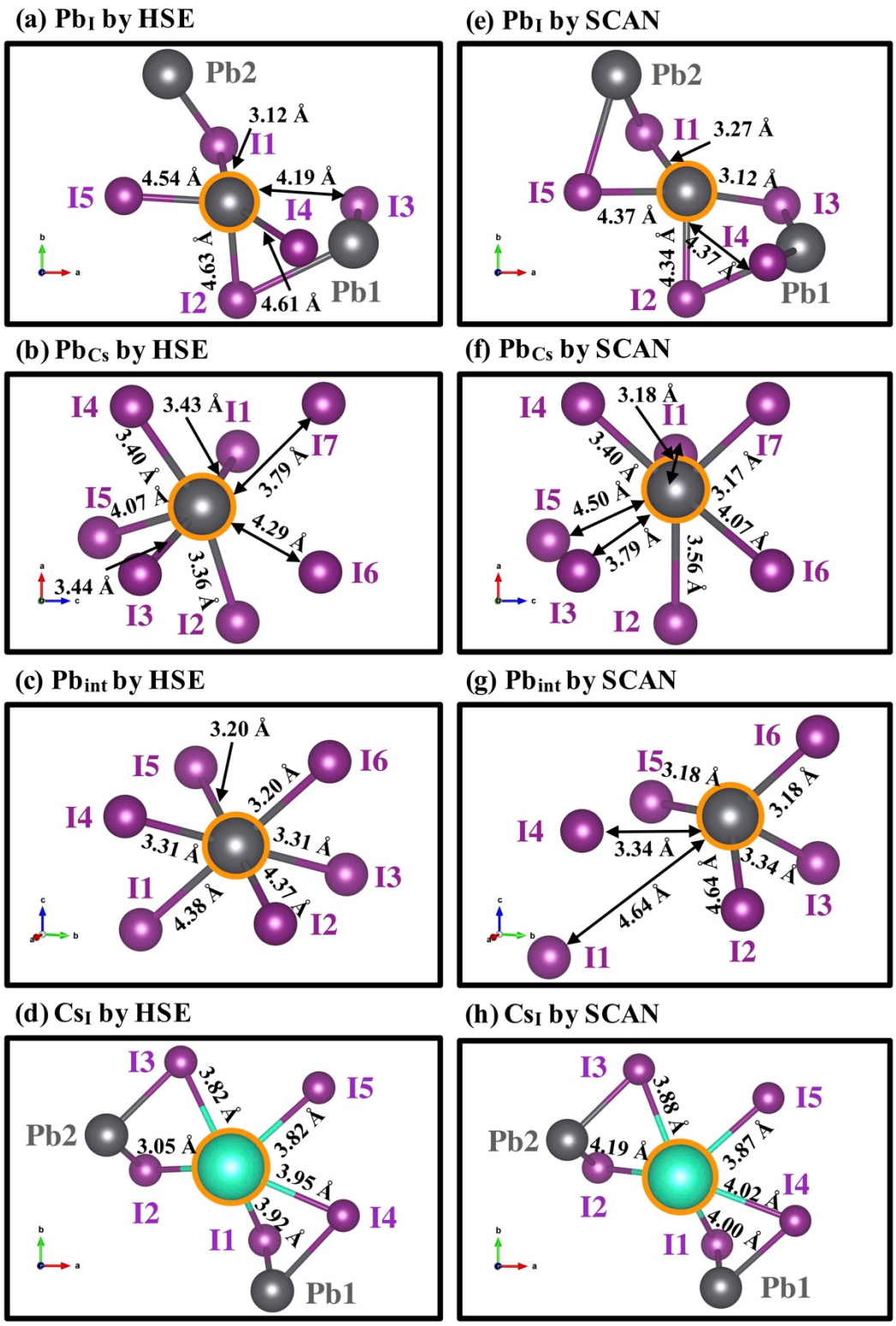

Fig. S2 Structural schematic illustration of neutral state of (a) Pb_I, (b) Pb_{Cs}, (c) Pb_{int} and (d) Cs_I by HSE functional and (e) Pb_I, (f) Pb_{Cs}, (g) Pb_{int} and (h) Cs_I by SCAN functional. The defect sites are trimmed by orange lines. The green, grey and purple spheres represent Cs, Pb and I atoms, respectively.

Note S5: Bandstructure of γ-CsPbI3

We derive an "orbital inverted" bandstructure by HSE functional, consistent with previous organic and inorganic LHPs. **Fig. S3** shows the band component analysis for VBM and CBM. A bandstructure with a direct bandgap of 1.72 eV located at Γ point is achieved. Furthermore, VBM mainly consists of antibonding hybridization between Pb 6s and I 5p orbitals, which elevates the band edge higher than pure atomic orbitals of Pb 6s or I 5p. The VBM state presents more of a I 5p character and CBM mainly arises from Pb 6p orbitals.

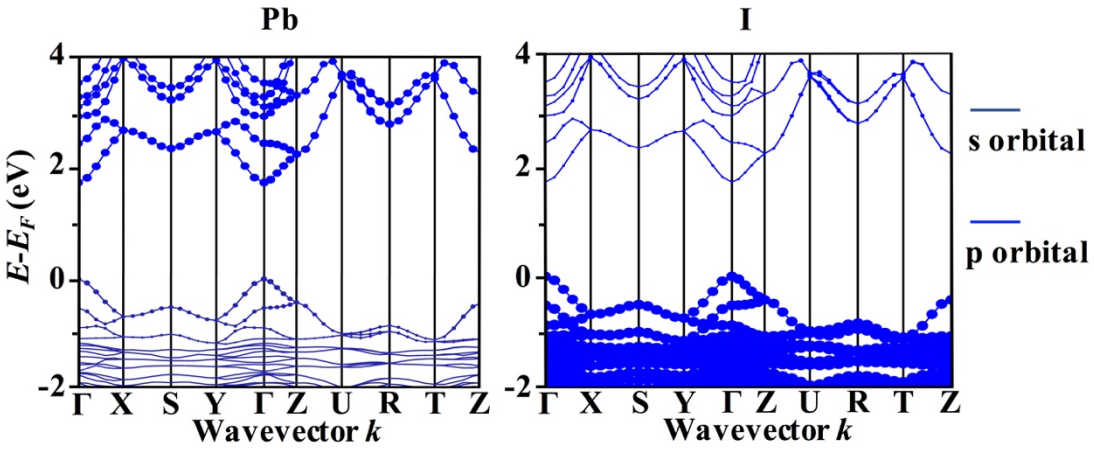

Fig. S3 Band component analysis for Pb-s, Pb-p and I-p orbitals.

Note S6: Structural deformation in Cs_{Pb}

Table S7. A list of distances d (Å) between Cs_{Pb} site cesium and neighboring iodines of 2+, 1+, 0 and 1– charge states. The same distances in the host lattice are also listed for comparison. The structural scheme is shown in **Fig. S4.**

Neighboring Iodine	d (Cs_{Pb}^{2+})	d (Cs_{Pb}^{1+})	d (Cs_{Pb}^{0})	d (Cs_{Pb}^{1-})	d (host)
I1	3.47	3.47	3.47	3.46	3.25
I2	3.47	3.47	3.47	3.47	3.25
I3	3.64	3.63	3.62	3.61	3.23
I4	3.64	3.63	3.62	3.61	3.23
I5	3.68	3.67	3.65	3.63	3.23
I6	3.69	3.67	3.66	3.64	3.23
Average	3.60	3.59	3.58	3.57	3.24

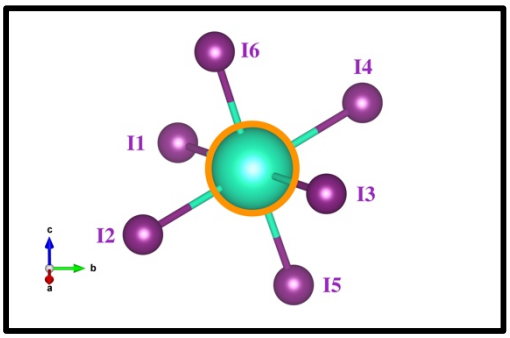

Fig. S4 Structure schematic of Cs_{Pb} by HSE functional.

References

[1] J. L. Lyons and C. G. Van de Walle, npj Comput. Mater. **3**, 12 (2017).

[2] A. Alkauskas, M. D. McCluskey, and C. G. Van de Walle, J. Appl. Phys. **119**, 181101 (2016).

[3] I. Vurgaftman and J. R. Meyer, J. Appl. Phys. **94**, 3675 (2003).